




# INBRX-106: a hexavalent OX40 agonist that drives superior antitumor responses via optimized receptor clustering

Nisha Holay <sup>1</sup>, Rashi Yadav,<sup>1,2</sup> Sae Jeong Ahn,<sup>3</sup> Melissa J Kasiewicz,<sup>1</sup> Anya Polovina,<sup>3</sup> Annah S Rolig <sup>1,2</sup>, Thi Staebler,<sup>3</sup> Bryan Becklund,<sup>3</sup> Noah D Simons,<sup>1</sup> Yoshinobu Koguchi,<sup>1,4</sup> Brendan P Eckelman,<sup>3</sup> Yaiza Diaz de Durana,<sup>3</sup> William L Redmond <sup>1</sup>

**To cite:** Holay N, Yadav R, Ahn SJ, *et al.* INBRX-106: a hexavalent OX40 agonist that drives superior antitumor responses via optimized receptor clustering. *Journal for ImmunoTherapy of Cancer* 2025;**13**:e011524. doi:10.1136/jitc-2025-011524

► Additional supplemental material is published online only. To view, please visit the journal online (<https://doi.org/10.1136/jitc-2025-011524>).

YDdD and WLR are joint senior authors.

Accepted 18 April 2025



© Author(s) (or their employer(s)) 2025. Re-use permitted under CC BY-NC. No commercial re-use. See rights and permissions. Published by BMJ Group.

<sup>1</sup>Earle A Chiles Research Institute, Providence Cancer Institute, Portland, Oregon, USA

<sup>2</sup>Oregon Health and Science University, Portland, Oregon, USA

<sup>3</sup>Inhibrx Biosciences Inc, La Jolla, California, USA

<sup>4</sup>The Ohio State University, Columbus, Ohio, USA

## Correspondence to

Dr William L Redmond;  
william.redmond@providence.org

Dr Yaiza Diaz de Durana;  
yaiza@inhibrx.com

## ABSTRACT

**Background** Immunotherapies targeting immune checkpoint inhibitors have revolutionized cancer treatment but are limited by incomplete patient responses. Costimulatory agonists like OX40 (CD134), a tumor necrosis factor receptor family member critical for T-cell survival and differentiation, have shown preclinical promise but limited clinical success due to suboptimal receptor activation. Conventional bivalent OX40 agonists fail to induce the trimeric engagement required for optimal downstream signaling. To address this, we developed INBRX-106, a hexavalent OX40 agonist designed to enhance receptor clustering independently of Fc-mediated crosslinking and boost antitumor T-cell responses.

**Methods** We assessed INBRX-106's effects on receptor clustering, signal transduction, and T-cell activation using NF- $\kappa$ B reporter assays, confocal microscopy, flow cytometry, and single-cell RNA sequencing. Therapeutic efficacy was evaluated in murine tumor models and *ex vivo* human samples. Clinical samples from a phase I/II trial (NCT04198766) were also analyzed for immune activation.

**Results** INBRX-106 demonstrated superior receptor clustering and downstream signaling compared with bivalent agonists, leading to robust T-cell activation and proliferation. In murine models, hexavalent OX40 agonism resulted in significant tumor regression, enhanced survival, and increased CD8<sup>+</sup> T-cell effector function. Clinical pharmacodynamic analysis in blood samples from patients treated with INBRX-106 showed heightened T-cell activation and proliferation, particularly in central and effector memory subsets, validating our preclinical findings.

**Conclusions** Our data establish hexavalent INBRX-106 as a differentiated and more potent OX40 agonist, showcasing its ability to overcome the limitations of conventional bivalent therapies by inducing superior receptor clustering and multimeric engagement. This unique clustering mechanism amplifies OX40 signaling, driving robust T-cell activation, proliferation, and effector function in preclinical and clinical settings. These findings highlight the therapeutic potential of INBRX-106 and its capacity to redefine OX40-targeted immunotherapy, providing a compelling rationale for its further clinical development in combination with checkpoint inhibitors.

## WHAT IS ALREADY KNOWN ON THIS TOPIC

⇒ Agonism of costimulatory receptors, such as OX40, is a therapeutic strategy complementary to immune checkpoint blockade but has not demonstrated significant therapeutic activity to date. However, prior conventional agonists evaluated in the clinic were bivalent antibodies that are inefficient at facilitating the trimeric engagement required for maximal receptor engagement and downstream signal activation.

## WHAT THIS STUDY ADDS

⇒ This study introduces INBRX-106, a novel hexavalent OX40 agonist designed to address the shortcomings of earlier-generation bivalent agonists. INBRX-106 enhances receptor clustering, signal transduction, and downstream activation resulting in significantly greater CD4<sup>+</sup> and CD8<sup>+</sup> T-cell proliferation and activation *in vitro* and *in vivo*. These effects translated into improved tumor regression and survival in murine models.

## HOW THIS STUDY MIGHT AFFECT RESEARCH, PRACTICE OR POLICY

⇒ This is the first study to provide evidence that a hexavalent OX40 agonist can achieve superior receptor clustering and signaling, leading to enhanced antitumor T-cell responses. These findings offer new mechanistic insights and establish a strong rationale for advancing INBRX-106 into clinical trials (NCT04198766), with the potential to redefine costimulatory receptor-targeted therapies in oncology.

## INTRODUCTION

Cancer immunotherapy seeks to amplify the antitumor cytotoxic potential of the immune system and has significantly transformed the oncology treatment landscape. Immune activation is regulated through a variety of costimulatory and inhibitory signals.<sup>1,2</sup> Treatment with immune checkpoint blockade (ICB) blocks inhibitory signals of checkpoint proteins such as cytotoxic T-lymphocyte associated protein 4 (CTLA-4), programmed cell

death protein 1 (PD-1), and programmed death-ligand 1 (PD-L1), thereby relieving T-cell inhibition and consequently enhancing antitumor activity.<sup>1,2</sup> To date, ICB of PD-(L)1, either alone or in combination, has resulted in improved survival and has become the standard of care across various indications.<sup>3,4</sup> Despite the success of ICB, not all tumor types and patients respond, and relapses occur frequently, highlighting the promise of finding more efficacious cancer immunotherapies.<sup>5,6</sup>

Following T-cell activation through the T-cell receptor and B7/CD28-mediated costimulation, further signaling is necessary to potentiate T-cell expansion, differentiation, and survival to support the generation of potent antitumor responses. Several groups have evaluated the ability of costimulatory receptor agonists to amplify T cell-mediated antitumor immunity.<sup>2</sup> Specifically, OX40 (CD134) is a costimulatory receptor belonging to the tumor necrosis factor receptor (TNFR) superfamily<sup>7,8</sup> and is expressed on activated immune cells, particularly CD4<sup>+</sup> and CD8<sup>+</sup> T cells, although it can be expressed by other immune cells including neutrophils and natural killer cells.<sup>7,9–11</sup> T-cell costimulation through OX40 significantly enhances T-cell proliferation, survival, and effector function.<sup>7,8,12</sup> Additionally, depending on the local microenvironment, OX40 agonism can affect the inhibitory function of regulatory Foxp3<sup>+</sup>CD4<sup>+</sup> T cells (T<sub>regs</sub>), potentially reducing their suppressive activity and contributing to a more robust and unhindered antitumor response.<sup>13–19</sup>

Despite ample preclinical data supporting OX40-induced T cell-mediated antitumor efficacy, previously evaluated OX40 agonists, primarily bivalent monoclonal antibodies (mAbs), have not shown significant clinical activity in patients.<sup>20–27</sup> One possible explanation for the lack of therapeutic efficacy is suboptimal receptor activation. Binding of the endogenous trimeric OX40 ligand to three OX40 molecules is essential for initiating downstream signaling;<sup>7,8</sup> however, super-clustering of costimulatory TNFRs, including OX40, is critical for optimal signaling.<sup>28–30</sup> Most OX40 agonists that have been evaluated clinically are bivalent mAbs, suggesting that candidates capable of promoting higher-order receptor clustering may be more likely to intensify the downstream signaling cascade and promote more potent antitumor immunity.<sup>2,28–31</sup>

INBRX-106 is a novel hexavalent OX40 agonist, comprised of six identical single domain antibodies (sdAbs) targeting OX40, joined end-to-end with a native human IgG1 Fc constant domain,<sup>32</sup> designed to overcome limitations of earlier-generation bivalent OX40. We hypothesize that a hexavalent agonist will further intensify the clustering of intracellular signaling components resulting in a greater magnitude of downstream signaling. This distinct hexavalent structure was engineered to allow INBRX-106 to engage multiple OX40 receptors and induce higher-order clustering, resulting in stronger activation of the OX40 costimulatory signaling pathway. Additionally, OX40 receptor clustering allows the intracellular

signaling components recruited by receptor activation to form a clustered network, potentially allowing signaling cooperativity between neighboring complexes.<sup>29</sup> Here, we present preclinical characterization of INBRX-106 and examine the impact of its higher valency on receptor clustering, downstream signaling, cell activation, proliferation, and subsequent antitumor activity. Finally, we also demonstrate robust biological activity in humans as indicated by costimulatory T-cell activity in patients treated with INBRX-106.

## METHODS

### Compounds

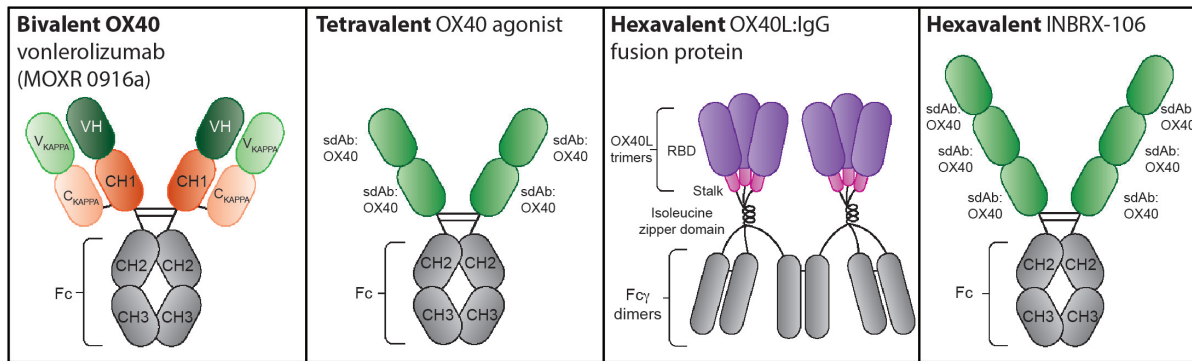
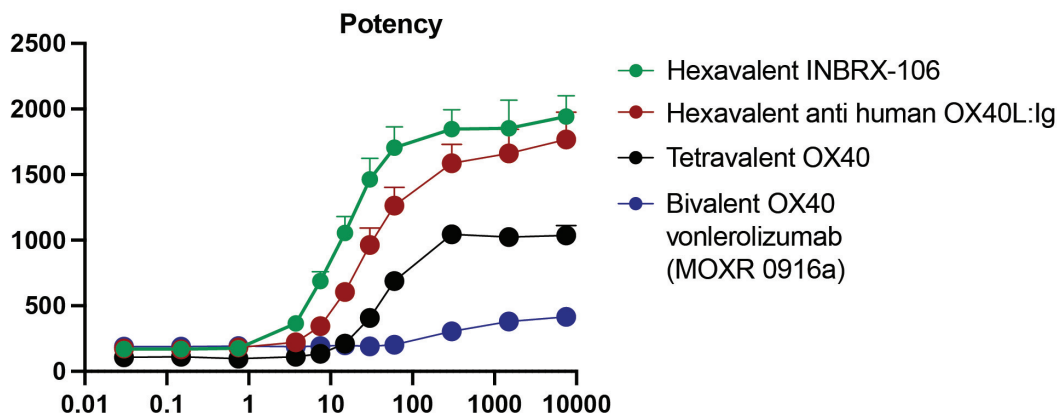
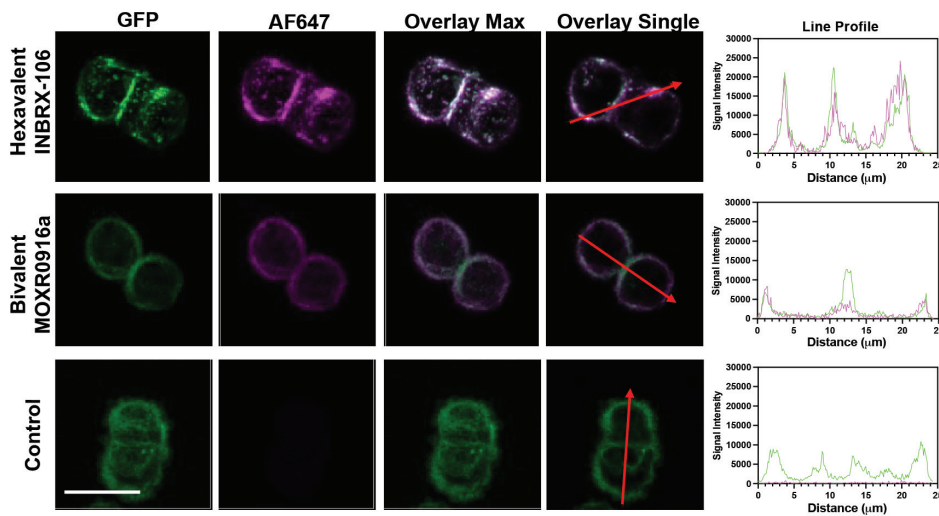
INBRX-106 and INBRX-106(m) (Inhibrx, La Jolla, California, USA) were used for human *in vitro* and murine *in vivo* studies, respectively, and are comprised of six identical OX40-targeting sdAbs (figure 1A) with a functional Fc domain (human, IgG1; murine, IgG2). An analog of human bivalent agonistic OX40 antibody vonlerolizumab (MOXR0916a) and a tetravalent version of INBRX-106 was also generated. The humanized hexavalent OX40L:IgG fusion protein links the extracellular domain of human OX40L to the Fc domain of a human IgG1 via a trimerizing isoleucine zipper domain (provided by Andrew Weinberg, EACRI).<sup>33</sup> Control rat IgG2a (Bio X Cell; Lebanon, New Hampshire, USA) and agonist murine anti-OX40 mAb (IgG2a; OX86 clone; Absolute Antibody; Oxford, UK) were diluted in phosphate-buffered saline (PBS) prior to use.

### Cell culture

Murine CT26 (BALB/c, ATCC; Manassas, Virginia, USA; RRID:CVCL\_7254) and MCA-205 (C57BL/6, ATCC; RRID:CVCL\_VR90) cells, and healthy donor human peripheral blood mononuclear cells (PBMCs) were cultured in Roswell Park Memorial Institute (RPMI)-1640 medium (Gibco; Miami, Florida, USA). Culture mediums were supplemented with 10% fetal bovine serum, 10 mmol/L HEPES (4-(2-hydroxyethyl)-1-piperazineethanesulfonic acid), 1% non-essential amino acids, 1% sodium pyruvate (Lonza; Basel, Switzerland), and 1% penicillin/streptomycin (Thermo Fisher; Waltham, Massachusetts, USA). Cell line identity was verified through monthly assessment of morphology and growth kinetics. Cell lines were tested annually using MycoAlert Mycoplasma Detection Kits (Lonza).

### PBMC isolation from healthy donors

Leukopaks from healthy donors were purchased from STEMCELL Technologies (Vancouver, California, USA) with prior institutional review board (IRB) approval. PBMCs were then isolated using Ficoll density gradient centrifugation. Whole blood was diluted with PBS/2% fetal bovine serum (FBS) and gently loaded onto a 50 mL conical tube containing 15 mL of Lymphoprep (STEMCELL). Cells were collected according to the Lymphoprep isolation protocol and resuspended in CryoStor

**A**

**B**

**C**


**Figure 1** INBRX-106 induces greater downstream signaling and receptor clustering over traditional OX40 agonists. (A) Schematic representing the design of OX40 agonists evaluated. Bivalent—in-house generated sequence analog of human bivalent IgG agonistic OX40 antibody vonlerolizumab (MOXR0916a); tetravalent OX40 agonist—four identical sdAbs targeting human OX40 joined end to end with an IgG constant domain; hexavalent OX40L:IgG fusion protein—a humanized OX40 agonist with a linked extracellular domain of human OX40L to the Fc domain of a human IgG1 via a trimerizing isoleucine zipper domain<sup>33</sup>; hexavalent INBRX-106 and its mouse surrogate—six identical sdAbs targeting OX40 (human or mouse) joined end to end with an IgG constant domain. (B) Potency of OX40 agonists on binding to OX40. Jurkat cells were treated with increasing concentrations of bivalent agonist (MOXR0916a), tetravalent agonist, and hexavalent agonists OX40L:Ig or INBRX-106 and then luciferase signal was measured. Graphs depict the mean±SEM. (C) Confocal microscopy imaging of cellular OX40 clustering. High-resolution confocal microscopy images of CHO cells expressing either OX40-GFP alone, AF647 secondary antibody, or an overlay are shown in the left, middle, and right, respectively. Pixel intensities of GFP (green) and AF647 (magenta) across the cell are shown on the line profile graphs. All images are representative of at least 10 images from three independent experiments. GFP, green fluorescent protein; sdAbs, single domain antibodies.



freezing media (Biolife Solutions, Bothell, Washington, USA). Cells were frozen at 1°C per hour overnight in a -80°C freezer using a Corning CoolCell Container and stored in liquid nitrogen. All samples analyzed were thawed at 37°C for 5 min and washed for further studies.

### **In vitro T-cell assays with healthy donor PBMCs**

PBMCs were resuspended in complete media and counted on an automated cell counter using trypan blue to exclude dead cells. Pan T cells or purified CD4<sup>+</sup> or CD8<sup>+</sup> T cells were used to evaluate proliferation and activation in the presence of OX40 agonism. EasySep Human T cell CD4<sup>+</sup> or CD8<sup>+</sup> isolation kits were used to enrich for desired populations following manufacturer's protocol (STEMCELL Technologies). Cells were resuspended at 20×10<sup>6</sup> cells/mL in labeling buffer with CellTrace Violet (Invitrogen) at a final dilution of 1:1,000. Cells were resuspended in complete media, suboptimally stimulated with anti-CD3 (OKT3) coated beads at a 2:1 T cell to bead ratio for 20 min and plated at 1.5×10<sup>5</sup> cells/well in 96-well U-bottom plates for pan T cells or 1×10<sup>5</sup> cells/well for purified CD4<sup>+</sup> or CD8<sup>+</sup> T cells. After 20 min incubation at room temperature (RT), OX40 agonists were added. Cells were incubated at 37°C and cell activation (online supplemental tablet S1) and proliferation were measured by flow cytometry after 4 days.

### **Cell-based OX40 activation assay**

Potency of OX40 agonists on binding to OX40 was evaluated using the OX40 Bioassay Propagation Model<sup>34</sup> (Promega; Madison, Wisconsin, USA), consisting of engineered Jurkat cells expressing human OX40 and a luciferase reporter driven by response to OX40 ligand/agonists. Cells were treated with serial dilutions of OX40 agonists for 5 hours at 37°C, 5% CO<sub>2</sub>. Luciferase production was quantified using commercial Bio-Glo Luciferase detection reagent. Luminescence signals were detected on a plate reader and relative luminescence units were plotted against corresponding OX40 agonist concentrations.

### **Confocal microscopy**

CHO cells, previously cultured in BalanCD CHO medium (Fuji; Tokyo, Japan), were transiently transfected with a plasmid driving expression of full-length human OX40 (RefSeq: NM\_003327.2) fused to green fluorescent protein (GFP) at the C-terminus. ExpiCHO-S cells were transfected (3:1) with PEI MAX high potency linear polyethyleneimine hydrochloride (Polysciences; Warrington, Pennsylvania, USA) and pCMV3-OX40-C-GFPspark (Sino Biological; Beijing, China). Each was diluted separately in Opti-MEM (1×) GlutaMAX Reduced Serum Medium (Gibco) before combining for 5 min at RT. PEI-DNA solution was added to cells and incubated for 14 hours (37°C; 8% CO<sub>2</sub>). OX40-expressing cells were identified based on GFP expression using an iQue Screener Plus (IntelliCyt; Albuquerque, New Mexico, USA) and sorted based on an

intermediate-to-high level of GFP expression, excluding the brightest cells.

To assess the effects of OX40 agonists on receptor clustering, 4×10<sup>4</sup> OX40-expressing cells were plated on an eight-well glass-bottom chamber (Ibidi; Grafelfing, Germany) previously coated with Collagen IV (Corning; Corning, New York, USA) as per manufacturer's recommendation. Cells were incubated with 5 nM or 25 nM of either hexavalent INBRX-106 or bivalent MOXR0916a, respectively, for 1 hour at 37°C, fixed with methanol-free 4% PFA (Electron Microscopy Sciences; Hatfield, Pennsylvania, USA), stained with AF546 Phalloidin (33 nM, Thermo Fisher; Waltham, Massachusetts, USA), and AF647-labeled secondary antibody (Jackson ImmunoResearch; West Grove, Pennsylvania, USA 1:200 for 30 min) before Hoechst nucleus staining (5 µg/mL for 10 min; Thermo Fisher). Cells were washed with PBS and overlaid with mounting medium (Ibidi). Images were acquired using a ZEISS LSM 980 confocal microscope and analyzed using ZEN analysis software. Imaging was done with 405, 488, 561, and 639 nm lasers at 1%, 0.5%, 1%, and 0.2% power, respectively, using 405, and 488/561/639 main beam splitters. A 20×0.8NA (numerical aperture) objective was used, and pixel size was set to 124 nm. Scan mode was set to unidirectional frame with a 1.34 µs pixel dwell time. Z-stacks spanning whole cells were collected with a 1.5 µm step size, with a pinhole set to 1 Airy unit. Fluorescence signals from DNA, GFP, cytoskeleton, and test articles were collected using four tracks with spectral ranges set to 428–499 nm, 490–570 nm, 570–597 nm, and 645–696 nm using gallium arsenide phosphate photomultipliers for visible range and a multialkali photomultiplier for infrared.

### **In vivo tumor studies**

6–8 weeks old female BALB/c (RRID:IMSR\_JAX:000651) and C57BL/6J (RRID:IMSR\_JAX:00064) mice obtained from Jackson Laboratories (Bar Harbor, Maine, USA), were maintained under specific pathogen-free conditions in the Earle A. Chiles Research Institute vivarium at Providence Portland Medical Center (Portland, Oregon, USA). Experimental procedures were performed according to the National Institutes of Health Guide for the Care and Use of Laboratory Animals and in accordance with the Institutional Animal Care and Use Committees. 1×10<sup>6</sup> (CT26 or MCA-205) tumor cells were inoculated subcutaneously in right flanks of wild-type mice. Tumor growth was monitored using two-dimensional (length×width) caliper measurements 2–3 times per week. Treatments began 8 days following implant, when tumors reached 40–60 mm<sup>2</sup>. Mice received control (rat IgG2a; 250 µg/dose; intraperitoneal (ip)), bivalent OX40 agonist (OX86 IgG2a; 250 µg/dose×2; ip), or hexavalent OX40 agonist (INBRX-106m; 10 µg/single dose; intravenous). Tumor size was measured until all animals reached a primary endpoint (tumor-free or total tumor burden >175 mm<sup>2</sup>). T-cell depletion experiments were performed using



200 µg anti-CD4 (clone GK1.5) or 200 µg anti-CD8 (clone 53–6.7).

### Tumor and lymph node collection and processing

Tumors were harvested 4 or 7 days post-treatment and digested in 1 mg/mL collagenase and 20 mg/mL DNase (Sigma; St. Louis, Missouri, USA) in serum-free RPMI-1640 for 30 min at RT. Tumor-infiltrating lymphocytes (TIL) were filtered through 70 µm nylon mesh (Cell Treat; Pepperell, Massachusetts, USA), washed with 10 mL 10% complete RPMI (cRPMI), and collected by centrifugation (1,500 rpm, 4 min). Pelleted cells were resuspended for staining and analysis by flow cytometry or single-cell RNA sequencing (scRNA-seq) (see below). Lymph nodes (LNs) were harvested 4 and 7 days post-treatment and processed to obtain single-cell suspensions. Red blood cells were lysed with ACK buffer (Lonza) for 2 min at RT. Cells were rinsed with cRPMI (Thermo Fisher) and resuspended and incubated with fluorescence-conjugated antibodies (online supplemental table S2) for 30 min at 4°C in the dark.

### Patient samples

Peripheral blood was collected from patients with advanced unresectable or metastatic solid tumors enrolled in a phase 1 dose-escalation clinical trial (NCT04198766). All human subjects were assessed for medical decision-making capacity using a standardized, approved assessment and voluntarily gave informed consent before being enrolled in the study. Patients were administered 0.1–3 mg/kg of INBRX-106 as a monotherapy or in combination with 200–400 mg of pembrolizumab (every 21 days). Blood samples were collected prior to treatment (C1D1), 15 days post-treatment (C1D15), or 21 days post-treatment (C1D21). Blood samples were drawn into BD Vacutainers according to the manufacturer's protocol. Fresh whole blood was evaluated with same-day analysis as described previously.<sup>35 36</sup> Briefly, heparinized whole blood was stained with a cocktail of antibodies to identify T-cell subsets (online supplemental table S3). For intracellular targets (ie, Ki-67), cells were fixed and permeabilized with eBioscience FOXP3/Transcription Factor Staining Buffer Kit (Thermo Fisher) followed by incubation with staining antibodies (online supplemental table S3). Samples were acquired with a BD LSRFortessa (BD Biosciences).

### Flow cytometry: antibodies and reagents

For TIL and LN phenotyping, single cell suspensions were stained for 30 min in the dark with combinations of surface markers (online supplemental table S2). Cells evaluated only for surface proteins or scRNA-seq were re-suspended in flow wash buffer containing PBS/2% FBS/5 mM EDTA or PBS/0.5% bovine serum albumin (BSA), respectively. All samples evaluated for intracellular proteins were stained with fixable viability dye LIVE/DEAD Green (Thermo Fisher) together with surface markers prior to fixation/permeabilization. Cells were fixed and permeabilized following manufacturer's

instructions (FOXP3/Transcription Factor Staining Buffer Set, Thermo Fisher) and stained with intracellular targets (online supplemental table S2). Flow cytometry data was acquired on a Cytex Aurora spectral cytometer (5L 16UV-16V-14B-10YG-8R). Spectral channels were unmixed on SpectroFlow software using fluorophore-specific single color controls using compensation beads (Thermo Fisher) and cells for viability dyes. All post-acquisition analysis was performed using FlowJo software (V.10.3) or OMIQ.

### Single-cell RNA sequencing

CT26 tumors were harvested from mice 7 days post-treatment (n=5/treatment group). scRNA-seq libraries were generated using the Chromium Single Cell 3' Library and Gel Bead Kit V.3.1 (10x Genomics; Pleasanton, California, USA). After reverse transcription, gel beads in emulsion were disrupted using the kit's recovery agent following manufacturer's instructions (10x Genomics). Barcoded complementary DNA was isolated and amplified by PCR (12 cycles). Following fragmentation, end repair, and A-tailing, sample indexes were added during index PCR (10x Genomics). Samples were resuspended at a concentration of 5 ng/µL and added in equal volumes to Illumina sequencing chips. scRNA-seq was performed using Illumina NovaSeq 6000. Data was analyzed using Seurat and BBrowserX (Bioturing). Briefly, for quality control, cells with the highest (top 0.2%) or lowest (bottom 0.2%) numbers of detected genes were excluded for downstream analyses. Genes of interest, or highly variable genes to be used for downstream analysis, were selected based on a dispersion value greater than 3. Dimensionality reduction by principal component analysis (PCA) was performed using variable genes. Uniform Manifold Approximation and Projection (UMAP) plots were generated based on PCA dimensions. Cell types were annotated with BioTuring's cell type ontology, identified by gating on relevant gene expression.

### Statistical analyses

Graphs show cumulative results with bar representing mean±SEM and each symbol representing results from independent experiments or experimental replicates. Statistical analyses were performed with Prism (V.10; GraphPad Software) or R to determine statistical significance as indicated using a Student's t-test, one-way analysis of variance (ANOVA), two-way ANOVA, or repeated measures ANOVA as appropriate along with Dunnett's multiple comparisons tests. Spearman's correlation was used to correlate peripheral blood lymphocyte and TIL populations with tumor size, and Kaplan-Meier plots and log-rank tests were used for tumor survival analysis. A p<0.05 was considered significant.

## RESULTS

### Enhancing OX40 signaling potency induced by multivalent OX40 agonists

Potent agonism of TNFRSF members, such as OX40, generally requires trimeric-ligand induced high-order receptor clustering on the cell membrane. Therefore, we hypothesized that multivalent engagement of OX40 would enable stronger downstream signaling. Canonically, OX40L-trimers bind to OX40 inducing receptor clustering resulting in downstream activation and translocation of nuclear factor kappa B (NF- $\kappa$ B) to the nucleus to facilitate interleukin-2 transcription, leading to lymphocyte expansion and differentiation. To investigate the impact of increased valency on this process, we used Jurkat cell lines expressing human OX40 and an NF- $\kappa$ B luciferase reporter.<sup>34</sup> The effect of OX40 agonists on receptor activation and downstream signaling was measured by luciferase expression. OX40-signaling reporter cells were incubated with either a bivalent OX40 agonist (MOXR0916a), a tetravalent agonist, or two different hexavalent agonists, OX40L:Ig fusion protein and INBRX-106 (figure 1A) and then luminescence was quantified. Conventional bivalent antibodies resulted in some OX40-induced activation, as previously reported.<sup>37</sup> However, tetravalent agonists led to improved signaling compared with bivalent agonism, and hexavalent agonism induced a further and marked increase in OX40-driven reporter activity (figure 1B). Overall, these results support the hypothesis that higher valency results in stronger activation of OX40 signaling.

### INBRX-106 induced higher clustering of the OX40 receptor

To dissect the mechanisms underlying the differences in downstream signaling potency between hexavalent and bivalent agents, we explored receptor clustering on CHO cells expressing a human OX40 extracellular domain coupled to GFP. Given that MOXR0916 was previously evaluated in the clinic we selected its analog, MOXR0916a, as a bivalent control to directly compare with INBRX-106 and evaluated their binding by confocal microscopy. Maximum intensity projection images revealed differences in receptor distribution patterns between the two agonists on binding. INBRX-106 induced distinct clusters while the bivalent MOXR0916a exhibited more dispersed staining throughout the same cell surface as revealed by the white gatherings in the overlay. Enhanced receptor clustering induced by the hexavalent agonist was demonstrated by high levels of co-occurrence of the two signals on the cell membrane, correlating with receptor clusters and internalization (figure 1C). The bivalent agonist elicited modest signal association on the cell membrane but did not lead to aggregation and accumulation of both signals inside the cell. As expected, control-treated cells showed no signal, and therefore no co-occurrence. Clustering was additionally evaluated by line profiles on single 1.5  $\mu$ m optical sections, which demonstrate a greater correlation of GFP-tagged receptor and INBRX-106, shown as spikes in these graphs. For the bivalent MOXR0916a, there was

receptor-antibody association on the cell membrane, but not intracellularly (figure 1C). Thus, while both agonists induce OX40 receptor clustering, INBRX-106 induces more robust receptor aggregation and internalization, which may promote increased signal accumulation and enhanced activity. Together, these data provide evidence that functional agonism correlates with distinct patterns of receptor clustering, with INBRX-106 generating more prominent OX40 clustering, thereby likely facilitating stronger downstream signaling.

### INBRX-106 enhances T-cell activation *in vitro*

OX40 agonism is known to increase T-cell proliferation, effector function, and survival. To measure the extent to which increased valence of OX40 agonism impacts T-cell function, we measured the proliferation and activation of T cells suboptimally activated with anti-CD3 in the presence of OX40 agonists. Changes in T-cell proliferation were measured by alterations in fluorescence intensity of the CTV stain/peak, where shifts below the undivided parental peak denote proliferation (online supplemental figure 1). In human pan-T cell cultures, increased CD4<sup>+</sup> and CD8<sup>+</sup> T-cell proliferation was observed after OX40 engagement, with maximum enhancement noted between 0.1–0.5 nM INBRX-106 and 10–100 nM OX40L fusion protein (hexavalent OX40L:Ig) (figure 2A–B). Furthermore, INBRX-106 induced statistically significant proliferation and activation effects at lower concentrations than the hexavalent OX40 fusion protein, when compared with the bivalent agonist. These oligomerization effects were also observed in a separate donor, although we were unable to include the OX40L fusion protein as the agent was no longer available (online supplemental figure 2A and B).

Activation was evaluated by surface expression of human leukocyte antigen (HLA)-DR, as this has been associated with T-cell activation in many disease models.<sup>38,39</sup> CD4<sup>+</sup> and CD8<sup>+</sup> T cells exhibited increased HLA-DR expression following hexavalent OX40 administration (figure 2A–B, online supplemental file 2A–B). To evaluate the direct effects of OX40 agonists on each T-cell subset, purified CD4<sup>+</sup> and CD8<sup>+</sup> T-cell populations were sorted from donor PBMCs, and proliferation was measured after suboptimal activation with anti-CD3 in the presence of OX40 agonists. As seen in the co-culture results, proliferation and activation markers were substantially enhanced on both purified T-cell populations with hexavalent treatment compared with traditional bivalent therapy. These data indicate INBRX-106 induces direct and potent agonistic effects on both CD4<sup>+</sup> and CD8<sup>+</sup> T cells, regardless of the differential receptor expression level in CD4<sup>+</sup> versus CD8<sup>+</sup> T cells (figure 2C–D, online supplemental figure 2C–D). In a system where OX40 expression is constant, our data suggests that valency is the driving factor in the differential activity between hexavalent and bivalent agonism.

The costimulatory activity of the hexavalent agonists exhibited a bell-shaped dose response curve, with maximal activity peaking between 0.1–10 nM for INBRX-106 and

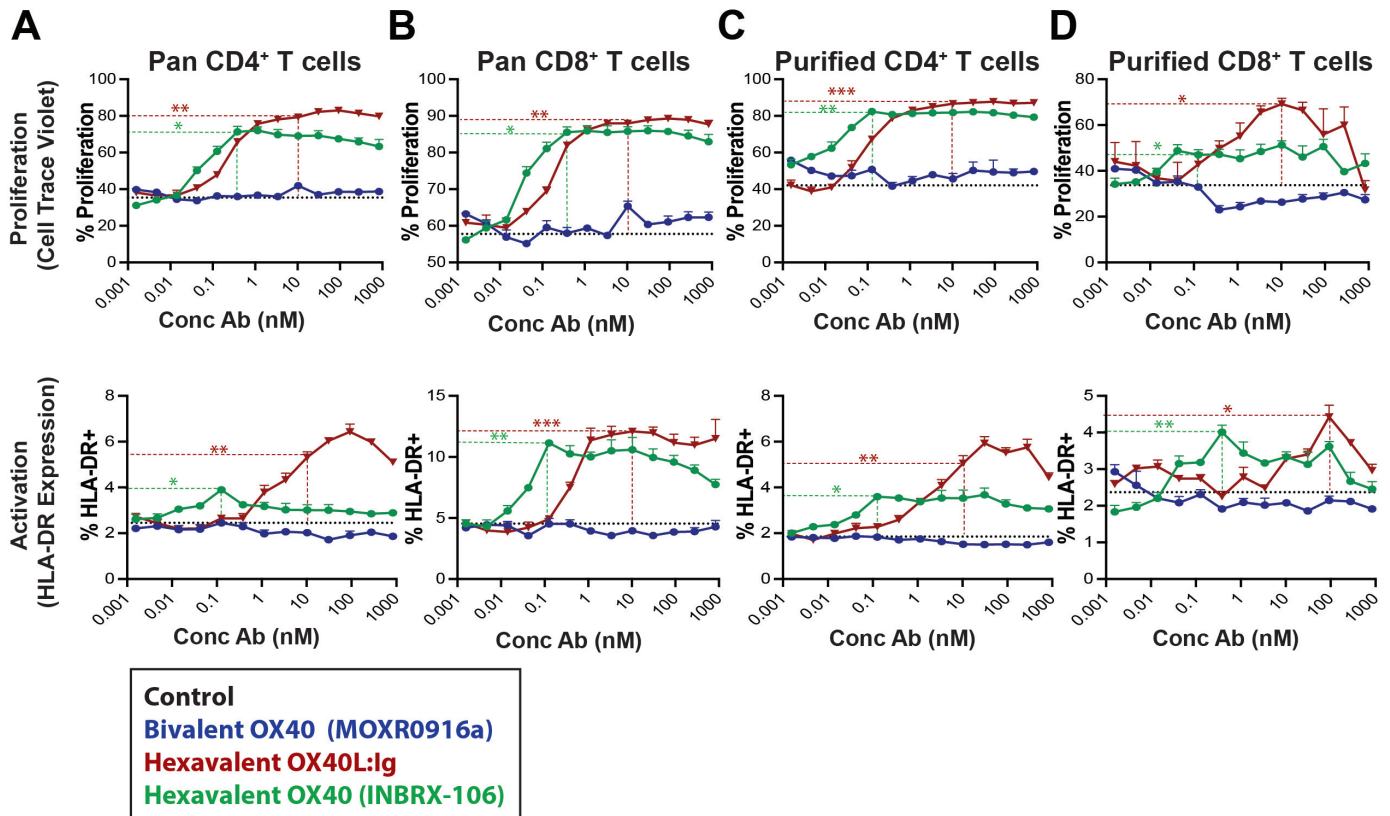


**Figure 2** OX40 agonism effects on T-cell proliferation and activation. CD4<sup>+</sup> and CD8<sup>+</sup> T cells enriched from healthy donor peripheral blood mononuclear cells were stained with a proliferation dye and suboptimally stimulated with anti-CD3 beads, either alone (dotted line) or in the presence of MOXR0916a (blue), hexavalent fusion protein (red), or INBRX-106 (green). (A) After 96 hours, CD4<sup>+</sup> T-cell proliferation in a pan T-cell culture was assessed. Activation of CD4<sup>+</sup> T cells within the mixed culture was evaluated by HLA-DR expression. (B) Proliferation of CD8<sup>+</sup> T cells in a pan T-cell culture was assessed following the same protocol as (A). Activation was evaluated by HLA-DR expression. (C–D) Purified CD4<sup>+</sup> or CD8<sup>+</sup> T cells were evaluated for proliferation and activation using the same protocol as (A–B). Graphs represent cumulative quantitative results of per cent proliferation after normalization (mean±SEM; n=3 healthy donors). \*p<0.05; \*\*p<0.01; \*\*\*p<0.001; \*\*\*\*p<0.0001 by two-way analysis of variance. Dotted lines represent statistical significance at indicated concentrations between bivalent OX40 (MOXR0916a) and hexavalent OX40L:Ig (red) or bivalent OX40 (MOXR0916a) and INBRX-106 (green).

OX40L Fc and declining at concentrations over 10 nM, suggesting that oversaturation of OX40 receptors does not result in added costimulatory activity above 100 nM. Overall, these results highlight the superior agonistic activity of INBRX-106 versus bivalent agonism consistent with the increased potency observed in the NF- $\kappa$ B reporter experiments. INBRX-106 also outperformed the bivalent antibody in activating human CD4<sup>+</sup> and CD8<sup>+</sup> T cells. Together, these data suggest a strong correlation between receptor clustering patterns and functional agonism, with INBRX-106 inducing more prominent clustering and, consequently, greater T-cell activation.

#### Hexavalent OX40 agonism elicited superior antitumor activity *in vivo*

OX40 agonists are thought to facilitate T-cell activation within the tumor-draining lymph nodes (tdLN), effectively priming the immune system for robust antitumor responses. Given OX40's pivotal role in boosting T-cell responses, we hypothesized that hexavalent OX40 agonism would further enhance T-cell priming and activation compared with the bivalent. Therefore, we investigated

the extent to which the hexavalent agonist improved the survival of MCA-205 (fibrosarcoma) or CT26 (colorectal adenocarcinoma) tumor-bearing mice. Mice were treated with control Ab, bivalent OX40 agonist mAb (OX86), or mouse surrogate hexavalent agonist (INBRX-106m) that was generated due to lack of rodent cross-reactivity of INBRX-106 (figure 3A). INBRX-106m contains an mIgG2a effector-enabled Fc, the mouse isotype most analogous to human IgG1. While INBRX-106m was valency, affinity, and activity matched to its human counterpart,<sup>32</sup> the difference in isotype may have additional impacts on activity not evaluated in this study. While treatment with the bivalent mAb had a lesser impact on tumor growth or survival (figure 3B–C), INBRX-106m treatment was well tolerated and led to decreased tumor size and significantly improved survival (figure 3B–C) in both models.

While CD4<sup>+</sup> and CD8<sup>+</sup> T cells transiently express OX40 following T cell receptor (TCR) stimulation, expression is higher on CD4<sup>+</sup> compared to CD8<sup>+</sup> T cells. Several studies have shown that OX40 agonist therapy directly targets CD4<sup>+</sup> and CD8<sup>+</sup> T cells,



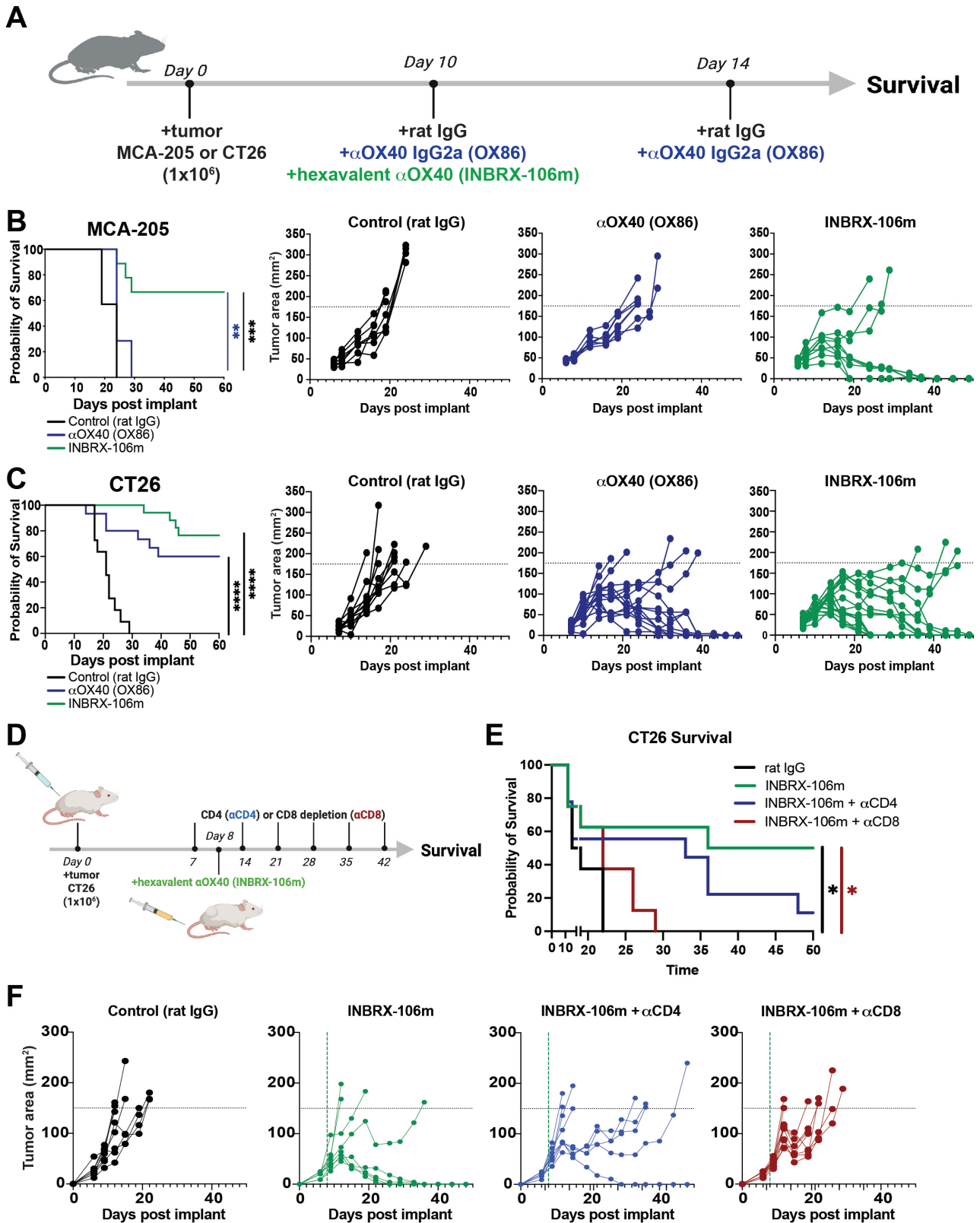


**Figure 3** Effect of OX40 agonism in murine tumor models. (A) Treatment schedule of MCA-205 (C57BL/6) or CT26 (BALB/c) mice ( $n=19$  mice/group), created with BioRender.com. Treatment began when tumor was established ( $\sim 7$  days after inoculation). Mice were treated with control rat IgG2a (250  $\mu\text{g}$ , intraperitoneal, 2 $\times$ ), bivalent agonist OX86 (250  $\mu\text{g}$ , ip, 2 $\times$ ), or hexavalent agonist INBRX-106m (10  $\mu\text{g}$ , intravenous, 1 $\times$ ). (B–C) Overall survival and tumor growth of (B) MCA-205 and (C) CT26 tumor-bearing mice treated with control, OX86, or INBRX-106m was evaluated. (D) Model, created with BioRender.com. CT26 tumor-bearing mice received anti-CD4, anti-CD8, or IgG isotype control at days 7, 14, 21, 28, 35, and 42 ( $n=10$  mice/group). INBRX-106m was administered at 10  $\mu\text{g}$  on day 8. (E) Overall survival and (F) tumor growth were determined. Graphs depict data from individual mice and survival was determined by the Mantel-Cox test. \* $p<0.05$ , \*\* $p<0.01$ , \*\*\* $p<0.001$ ; \*\*\*\* $p<0.0001$ .

highlighting the importance of both cell types in mediating the effects of these therapies.<sup>40–43</sup> To investigate the role of these subsets, we depleted CD4<sup>+</sup> or CD8<sup>+</sup> T cells and found that INBRX-106m efficacy was highly dependent on CD8<sup>+</sup> T cells, while the absence of CD4<sup>+</sup> T cells only partially reduced its effects (figure 3D–F, online supplemental figure D–F). This suggests that INBRX-106m can effectively engage and activate CD8<sup>+</sup> T cells to control tumor growth, even with limited CD4<sup>+</sup> T-cell help and despite CD8<sup>+</sup> T cells' lower levels of OX40 expression.

### INBRX-106m induced robust CD8<sup>+</sup> T-cell expansion and effector differentiation in murine tumor models

Our data demonstrated that INBRX-106m induced more potent systemic antitumor responses than bivalent anti-OX40 (OX86). To understand the

pharmacodynamic effects of this response, we characterized the phenotypic and functional status of effector Foxp3<sup>-</sup> CD4<sup>+</sup> (T<sub>eff</sub>), regulatory Foxp3<sup>+</sup> CD4<sup>+</sup> (T<sub>reg</sub>), and CD8<sup>+</sup> T cells post-treatment. CT26 tumor-bearing mice were treated with control IgG, bivalent OX86, or hexavalent INBRX-106m. LNs and TILs were harvested 4 and 7 days post-treatment and T-cell responses were evaluated via flow cytometry (figure 4A). INBRX-106m significantly expanded CD8<sup>+</sup> T cells within the tumor at day 7 and greatly increased the frequency and proliferation of T cells within the LN (figure 4D, online supplemental figure 3 and 4). Remarkably, while we observed a large CD8<sup>+</sup> T-cell population following INBRX-106m treatment, this did not appear to be attributed to tumor-intrinsic proliferation, as we did not observe a concomitant increase in Ki-67 expression within the expanded

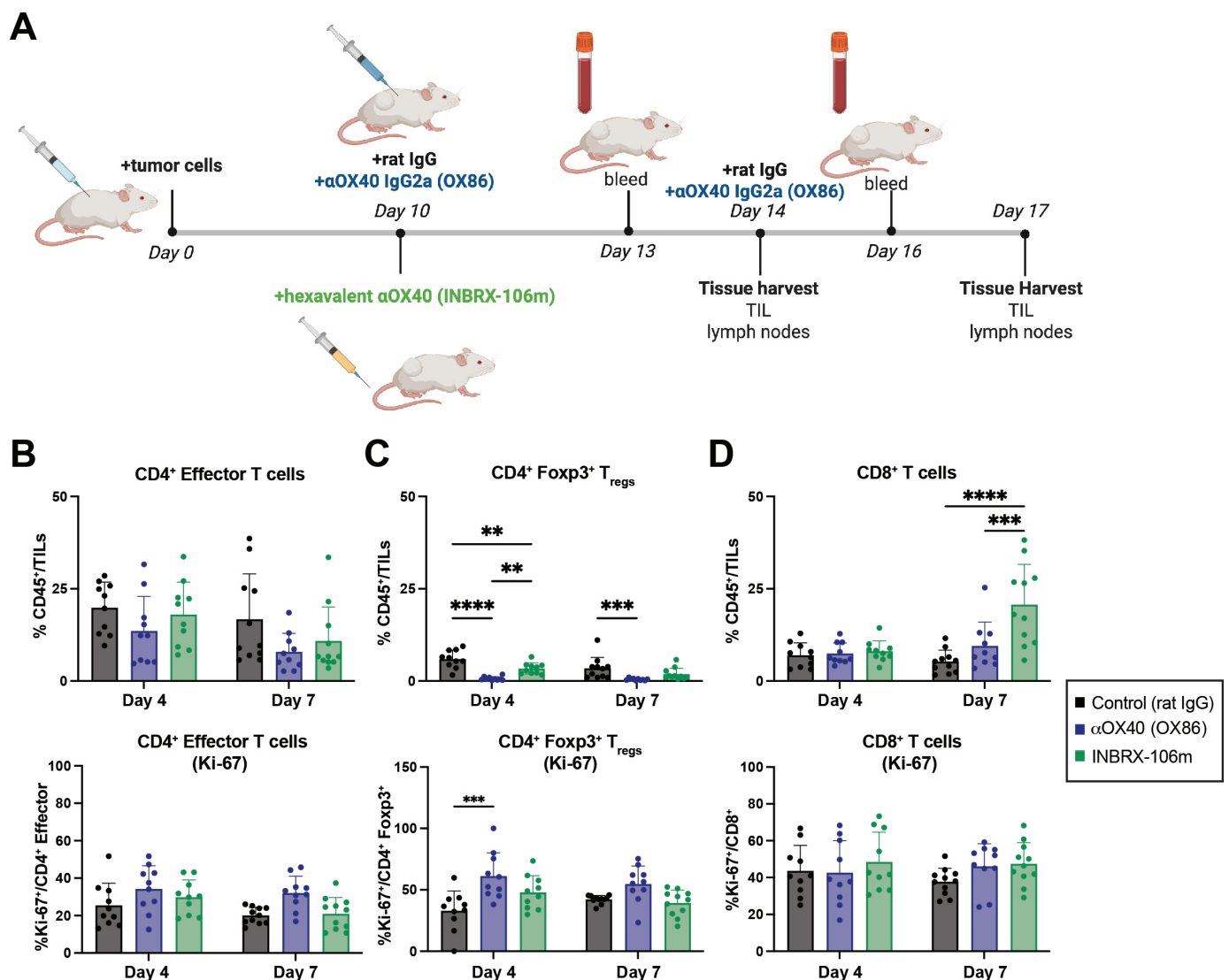


**Figure 4** Hexavalent agonism increases CD8<sup>+</sup> T-cell frequency and decreases T<sub>reg</sub> frequency. (A) Model, created with BioRender.com. (B) Flow cytometry analysis of TIL effector CD4<sup>+</sup> T cells (B), Foxp3<sup>+</sup> CD4<sup>+</sup> T<sub>regs</sub> (C), and CD8<sup>+</sup> T cells (D) including the frequency of CD45<sup>+</sup> T cells (top row) and Ki-67 expression (bottom row). Graphs depict cumulative results (mean±SEM) from two independent experiments including control (n=8), bivalent OX86 (n=9), and INBRX-106m (n=12). \*p<0.05; \*\*p<0.01; \*\*\*p<0.001; \*\*\*\*p<0.0001 by one-way analysis of variance. TIL, tumor-infiltrating lymphocyte; T<sub>reg</sub>, regulatory T cell.

CD8<sup>+</sup> T-cell population. We therefore examined tdLNs and peripheral blood (online supplemental figure 5) to determine whether the enhanced TIL frequency reflects efflux from the LN. Surprisingly, we observed decreased CD8<sup>+</sup> T-cell frequency in the tdLN, but a corresponding increase in proliferation (Ki-67) (online supplemental figure 4A and B), suggesting LN CD8<sup>+</sup> T cells are more proliferative but on OX40 agonist therapy, may leave the secondary lymphoid organs to traffic to the tumor site.

We also evaluated the effects of higher valency treatment on CD4<sup>+</sup> T<sub>eff</sub> and T<sub>regs</sub>. Analogous to its effects on CD8<sup>+</sup> T cells, INBRX-106m showed a trend of increasing CD4<sup>+</sup> T<sub>eff</sub> proliferation as compared with controls in the tumor and LN (figure 4B, online supplemental figure 4A-B). Additionally, T<sub>regs</sub> were significantly depleted in LN and TIL following bivalent OX86 treatment, but only slightly reduced with INBRX-106m (figure 4C and online supplemental figure A-B). Ex vivo analyses of cytokine production revealed enhanced interferon (IFN)- $\gamma$  and TNF- $\alpha$  production after INBRX-106m treatment compared with control and bivalent treatments in the LN (online supplemental figure C-D). These analyses indicate that hexavalent INBRX-106m therapy results in enhanced T-cell activation and T cell-mediated antitumor activity, culminating in tumor regression.

#### Single-cell transcriptomic profiling of CD45<sup>+</sup> cells in the tumor microenvironment (TME) revealed unique features following hexavalent treatment

Given that CD8<sup>+</sup> T cells play an important role in the efficacy of INBRX-106m, and the associated changes in expansion and differentiation of these cells, we sought to investigate the impact of INBRX-106 on the transcriptional profile of CD8<sup>+</sup> T cells using scRNA-seq. CD45<sup>+</sup>CD11b<sup>-</sup> cells were isolated from tumors 7 days post-treatment and processed for scRNA-seq. We sequenced 8706 cells from controls, 8,476 cells from bivalent OX86, and 7,546 cells from mice treated with INBRX-106m, achieving over 90,000 reads per cell. UMAP analysis and unbiased clustering identified 15 distinct clusters, including three CD8<sup>+</sup> T-cell clusters, two effector CD4<sup>+</sup> T clusters, and one T<sub>reg</sub> cluster (figure 5A). Cellular distribution across these clusters confirmed our earlier observations that mice receiving INBRX-106m have an increased frequency of CD8<sup>+</sup> T cells and a decreased frequency of T<sub>regs</sub> compared with controls (figure 5B).

Additionally, we sought to determine whether the observed changes in gene expression were specifically caused by INBRX-106m's hexavalent structure and enhanced receptor clustering, or if they were a general effect of OX40 agonism. Many genes associated with differentiated tumor-specific CD8<sup>+</sup> T cells, including *Ifng*, *Gzmb*, *Prf1*, *Tox*, *Pdcd1*, and *Lag3*, were increased in the effector CD8<sup>+</sup> T population of hexavalent-treated mice (figure 5C-D). Analyses of

CD8<sup>+</sup> T-cell clusters demonstrated that INBRX-106m decreased expression of 99 genes in comparison to bivalent OX86 treatment (figure 6A and D-I), and increased expression of 219 genes compared with the OX86 agonist (figure 6B and D-I). Graphical Gene Set Enrichment Analyses also indicated hexavalent agonism preferentially activates pathways involved in signal receptor binding, cytokine activity, and leukocyte chemotaxis compared with the bivalent OX86 (figure 6C).

#### Pharmacodynamic effects of INBRX-106 in patients with cancer

We next sought to validate these observations in samples collected from patients treated with INBRX-106. Our goal was to determine if the T-cell proliferation and activation effects observed in our preclinical models were also evident in a clinical setting. The clinical development of INBRX-106, as a monotherapy and in combination with anti-PD-1 (pembrolizumab), provided an opportunity to address this question. We analyzed a total of 48 fresh peripheral whole blood samples from 16 patients enrolled in a phase I/II clinical trial (NCT04198766) over one complete 21-day cycle of INBRX-106 treatment, either alone or in combination with anti-PD-1. In this trial, patients received INBRX-106 every 3 weeks (online supplemental table S4 and S5). We obtained samples from selected patients at three different time points: pretreatment (C1D1), 15 days later (C1D15), and 21 days following their initial treatment (C1D21). We did not observe significant changes pretreatment to post-treatment in the overall frequency of CD3<sup>+</sup>, CD4<sup>+</sup>, or CD8<sup>+</sup> T cells (online supplemental figure 6). However, we observed significant increases in proliferation (Ki-67) among patients receiving combination therapy, which was consistent with our murine data (figure 7A-C).

Akin to our findings from the *in vitro* analyses, we also observed increased expression of the activation markers CD38 and HLA-DR on T cells following INBRX-106 treatment. Activation was sustained with INBRX-106 alone and in combination with pembrolizumab, although the effect was more pronounced following combination treatment (figure 7D-F). Next, we examined the effects on naïve (CD45RA<sup>+</sup>CCR7<sup>+</sup>), central memory (CD45RA<sup>-</sup>CCR7<sup>+</sup>), Temra (CD45RA<sup>+</sup>CCR7<sup>-</sup>), and effector memory (CD45RA<sup>-</sup>CCR7<sup>-</sup>) subsets (figure 7G-H). In monotherapy and combination-treated patients, CD4<sup>+</sup> and CD8<sup>+</sup> central memory, Temra, and effector memory T cells showed drastic increases in proliferation after initial INBRX-106 treatment (figure 7G-H). Together, these data studies highlight the superior potency of INBRX-106. By optimizing receptor clustering, INBRX-106 more effectively enhances T-cell proliferation compared with traditional bivalent agonists, *in vitro* and *in vivo*.



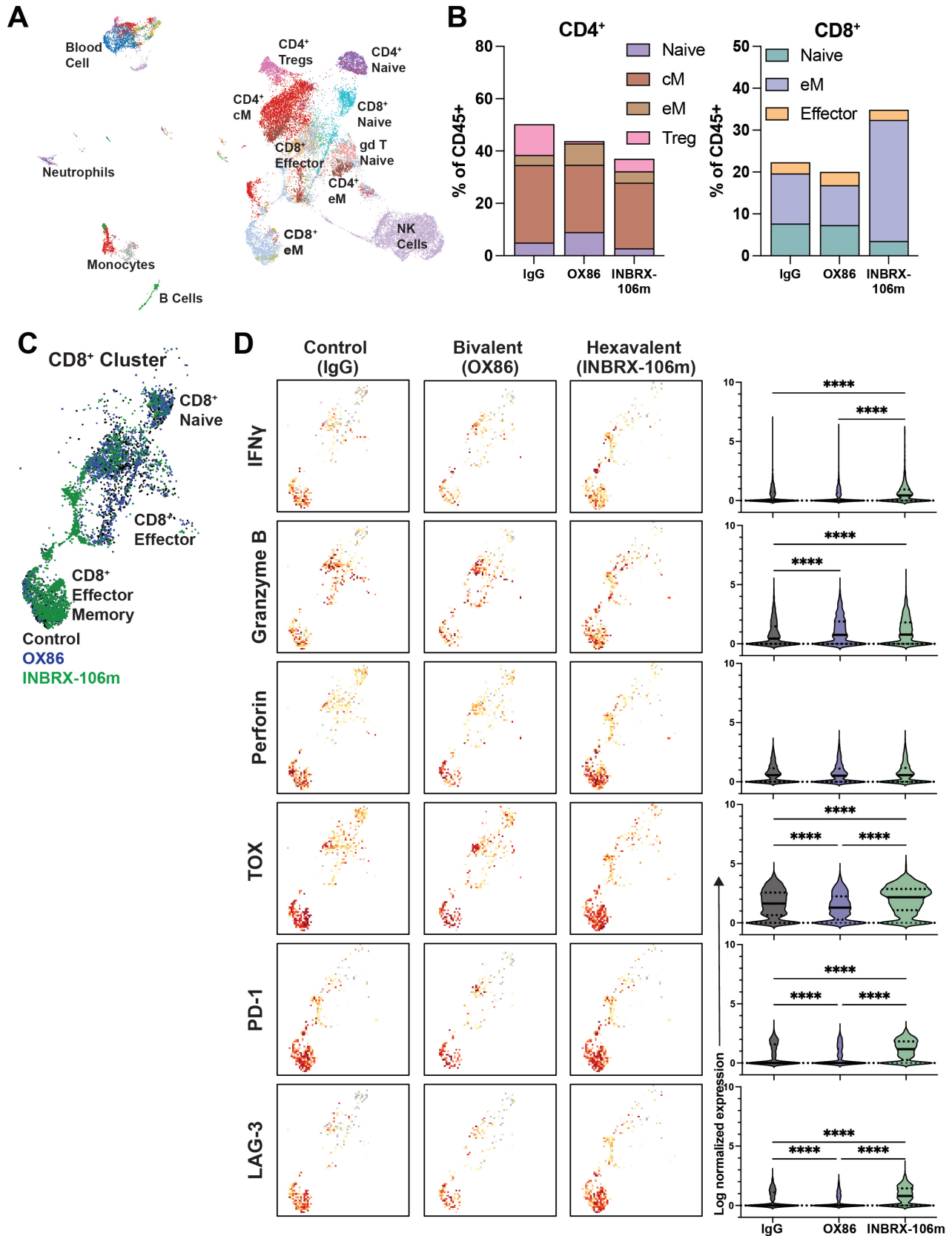


**Figure 5** Single-cell RNA-seq indicates activated clusters of CD8<sup>+</sup> T cells within hexavalent-treated murine tumors. Five tumors from each treatment group were pooled for scRNA-seq. (A) UMAP of scRNA-seq data. (B) Cell distribution across scRNA-seq clusters. (C) UMAPs of CD8<sup>+</sup> T-cell clusters and (D) activation and exhaustion markers. Dot color represents gene expression level. Violin plots show the distribution of expression of indicated genes comparing cells from control, bivalent (OX86), or hexavalent (INBRX-106m)-treated mice. \*\* $p < 0.01$ ; \*\*\* $p < 0.001$ ; \*\*\*\* $p < 0.0001$  by Student's t-test. scRNA-seq, single-cell RNA sequencing; Treg, regulatory T cell; UMAP, Uniform Manifold Approximation and Projection.

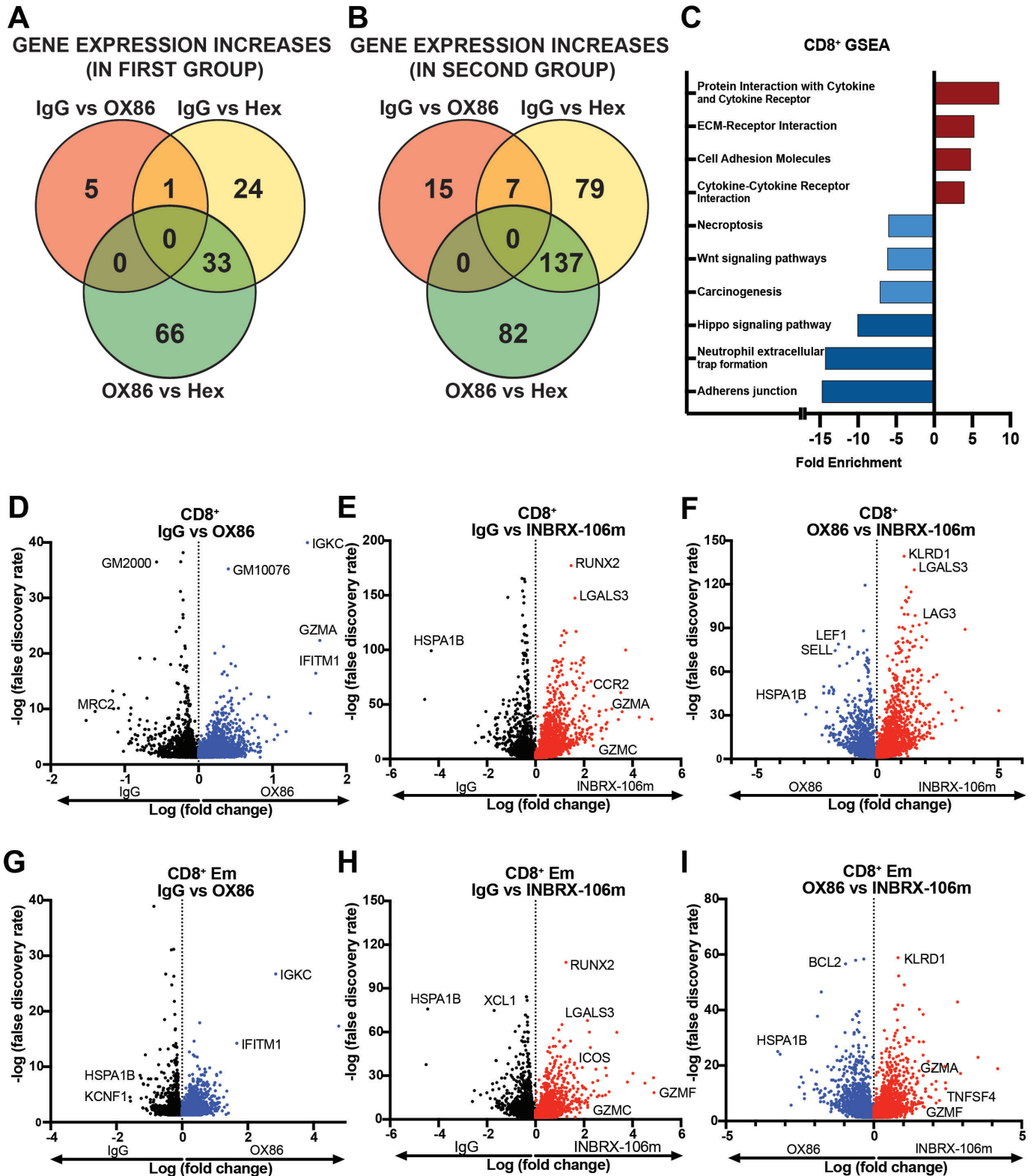


**Figure 6** Gene expression changes correspond with increased immunity pathways. (A) Venn diagram of differentially expressed genes that are increased in the first group of each comparison (IgG, IgG, and OX86 for the red, yellow, and green circles, respectively) relative to the second treatment group. Numbers in each circle represent the amount of differentially expressed genes between the indicated groups. (B) Venn diagram of differentially expressed genes that are increased in the second group of each comparison (OX86, Hex, and Hex for the red, yellow, and green circles, respectively) relative to the first treatment group. (C) Gene Ontology (GO) pathway enrichment analysis and the Gene Set Enrichment Analysis (GSEA) of differentially-expressed genes in the CD8<sup>+</sup> T-cell cluster between OX86 and the INBRX-106m treated groups. (D–I) Volcano plots of differentially expressed genes of indicated T-cell subtypes and treatments. ECM, extracellular matrix.

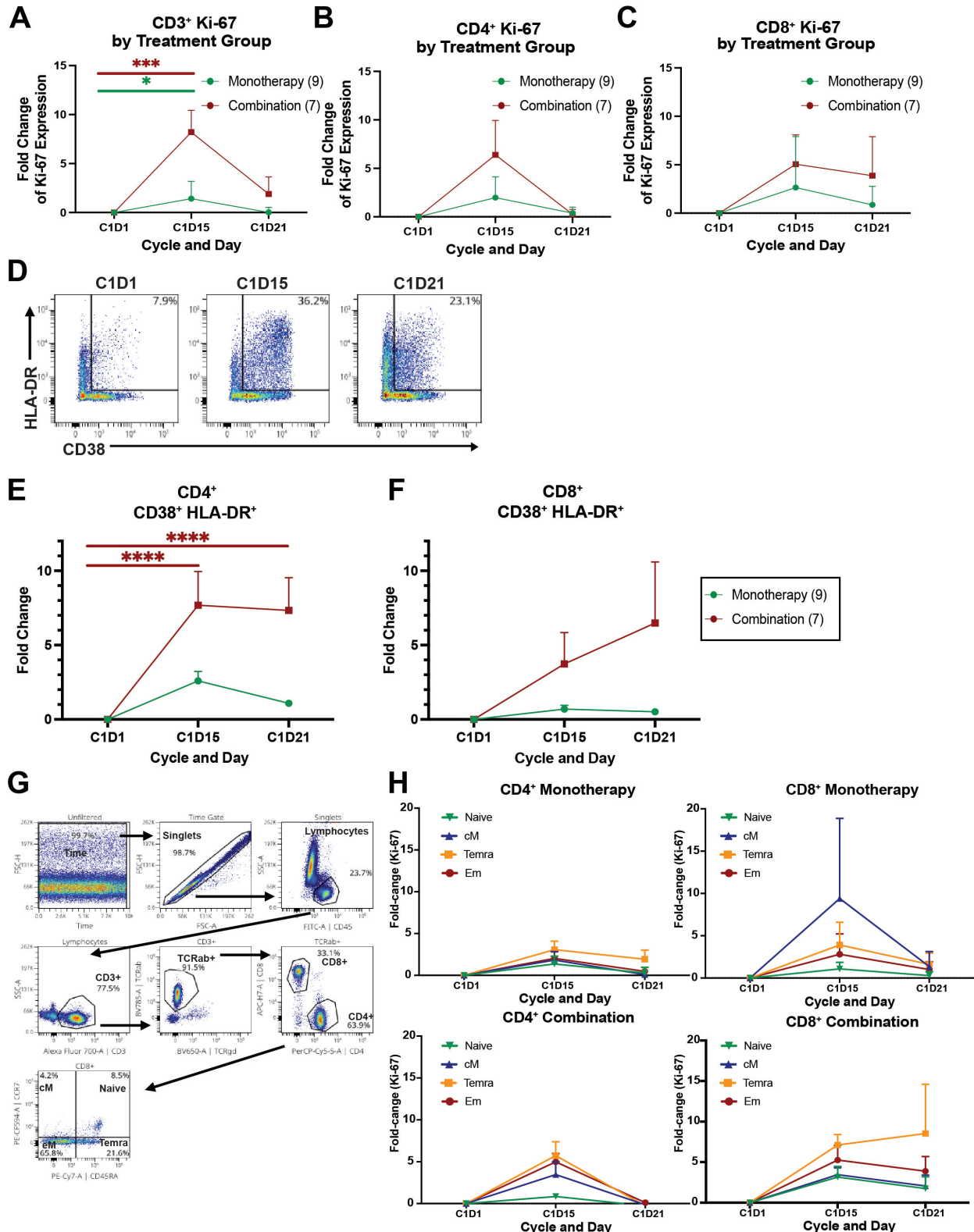


**Figure 7** INBRX-106 induces rapid changes in proliferation and activation of T cells from patients peripheral blood mononuclear cells were isolated at baseline (C1D1), 15 days post-treatment (C1D15), and 21 days post-treatment (C1D21) from patients receiving INBRX-106 monotherapy or in combination with pembrolizumab. (A–C) Immune cell proliferation was assessed by Ki-67 expression. All patients were normalized to their own baseline. (D) Representative flow cytometry plots showing the gating strategy of activated CD38<sup>+</sup>HLA-DR<sup>+</sup> CD8<sup>+</sup> T cells. (E–F) Quantification of activated (CD38<sup>+</sup>HLA-DR<sup>+</sup>) CD4<sup>+</sup> or CD8<sup>+</sup> T cells in patients receiving INBRX-106±pembrolizumab. (G) Gating strategy to analyze naïve (CD45RA<sup>+</sup>CCR7<sup>+</sup>), central memory (CD45RA<sup>-</sup>CCR7<sup>+</sup>), effector memory (CD45RA<sup>-</sup>CCR7<sup>-</sup>), or Temra (CD45RA<sup>+</sup>CCR7<sup>-</sup>) T cell subsets. (H) Proliferation (Ki-67) was evaluated in each memory subset in patients receiving monotherapy or combination therapy. Graphs depict the mean±SEM; \*p<0.05; \*\*\*p<0.001; \*\*\*\*p<0.0001 by unpaired Student's t-test.



## DISCUSSION

The data presented in this study highlight the transformative potential of INBRX-106, a novel hexavalent OX40 agonist, in potentiating the use of higher valency for enhanced clinical outcome. While bivalent mAbs were employed due to their ability to mimic cell signaling properties of natural ligands, clinical OX40 agonists, like MOXR0916 (Genentech), PF-04518600 (Pfizer), and INCAGN01949 (Incyte) among others have shown limited efficacy even in combination with checkpoint inhibitors.<sup>44</sup> These shortfalls may be attributed to bivalent mAbs inability to achieve higher-order receptor clustering essential for maximal OX40 activation. In contrast, OX40's natural trimeric ligand induces receptor hyperclustering, which is critical to fully activate downstream signaling (eg, NF- $\kappa$ B) and drive robust T-cell responses, while bivalent mAbs rely on suboptimal or inconsistent *in vivo* crosslinking.

INBRX-106 overcomes this limitation through its hexavalent design, featuring six sdAbs targeting OX40 on a human IgG1 Fc backbone, enabling trimeric receptor engagement and autonomous clustering without external crosslinking, leading to enhanced receptor activation, stronger T-cell responses, and improved antitumor efficacy. In both preclinical models and clinical samples, INBRX-106 consistently drove sustained CD4<sup>+</sup> and CD8<sup>+</sup> T-cell proliferation and activation, resulting in more pronounced tumor regression and improved survival. These findings reaffirm the importance of receptor clustering for TNFR superfamily agonists and introduce a new paradigm for optimizing costimulatory receptor activation. Furthermore, INBRX-106's hexavalent design helps to achieve the critical balance between potency and safety—an essential consideration for TNFR superfamily agonists. Unlike CD28, whose broad expression led to severe toxicities (eg, TGN1412), OX40 is limited to activated T cells, offering a more favorable therapeutic window.<sup>45–47</sup> This selectivity, combined with enhanced potency at lower doses, positions INBRX-106 as a safer and more effective alternative.

While the preclinical data demonstrate that hexavalent OX40 agonism leads to robust receptor clustering and signaling, the effectiveness may be influenced by T<sub>regs</sub> within the TME. Although some studies show that OX40 agonism reduces T<sub>reg</sub>-mediated suppression,<sup>48</sup> INBRX-106 shows modest effects on T<sub>reg</sub> depletion compared with bivalent agonists. Given that INBRX-106m efficacy may involve enhanced CD8<sup>+</sup> T-cell activity and decreased T<sub>reg</sub> suppression function, further research is needed to clarify the influence of T<sub>regs</sub> in mediating the efficacy of hexavalent OX40 agonists. Additionally, INBRX-106's efficacy may vary with TME differences, including OX40 expression levels on other immune cells. Our preliminary analyses into other cell types that express OX40, such as natural killer cells, revealed increases in frequency and proliferation, suggesting INBRX-106 may have complementary effects on non-T-cell antitumor responses (online supplemental figure 7). Evaluating longitudinal

clinical data from paired tumor biopsies and peripheral blood samples will be essential to further characterize INBRX-106's pharmacodynamic effects, including T-cell trafficking, immune cell exhaustion, and TIL dynamics. scRNA-seq studies are also underway to refine our understanding of INBRX-106's modulation of distinct immune cell populations and their functional states within the TME. Additionally, combining INBRX-106 with checkpoint inhibitors like anti-PD-1 or anti-CTLA-4 could yield complementary mechanisms of action, enhancing both the priming and effector phases of the antitumor response.<sup>27 40 49 50</sup>

In conclusion, INBRX-106 represents a significant advancement in OX40-targeted immunotherapy, offering a first-in-class approach to overcome the limitations of prior bivalent agonists. By enabling superior receptor clustering and downstream signaling, INBRX-106 enhances antitumor immunity. These findings provide a compelling rationale for further clinical development of INBRX-106, both as a monotherapy and in combination with other immunotherapeutic agents, with the potential to redefine the therapeutic landscape for OX40 agonists.

X Annah S Rolig @annahrolig

**Acknowledgements** We would like to thank the EACRI Immune Monitoring Laboratory, EACRI Flow Cytometry Core, EACRI Bioinformatics Core, and EACRI Cancer Research Animal Division for their technical assistance. We would also like to thank Rajay Pandit for his expertise and meticulous work in performing the transfection and sorting of CHO cells, as well as Dr. Zbigniew Mikulski of the LJI Microscopy Core for his expert assistance with our research.

**Contributors** Conceptualization: NH, RY, YK, BPE, YDdD, WLR. Methodology: NH, RY, BB, SJA, NDS, MJK, AP, ASR, TS, YK, BPE, YDdD, WLR. Formal analysis: NH, RY, SJA, NDS, MJK, AP, ASR, TS, YK, YDdD. Investigation: NH, RY, SJA, BB, NDS, MJK, AP, TS, YK, YDdD. Visualization: NH, RY, YDdD, NDS, ASR, YK. Funding acquisition: WLR. Project administration: YDdD, WLR. Supervision: YDdD, WLR. Writing—original draft: NH, RY, YDdD, WLR. Writing—review and editing: NH, RY, BB, NDS, MJK, ASR, YK, YDdD, WLR. Guarantor: WLR.

**Funding** Funding was provided by an Inhibrx research grant, the M. J. Murdock Charitable Trust, and the Providence Portland Medical Foundation (WLR). Confocal microscopy ZEISS LSM980 was funded by NIH grant S10 OD030417.

**Competing interests** NH, RY, NDS, MJK, and ASR have no competing interests. YDdD, BPE, BB, SJA, AP, and TS are employed by Inhibrx Biosciences Inc. BPE is a shareholder of Inhibrx Biosciences Inc. and an inventor on patents and patent applications related to INBRX-106. YK: Research support from Shimadzu. WLR: Research support from Inhibrx, Bristol-Myers Squibb, Veana Therapeutics, Shimadzu, Galecto, and CanWell Pharma. Patents/Licensing fees: Galectin Therapeutics. Scientific Advisory Boards: Vesselon, Medicenna, and Veana Therapeutics.

**Patient consent for publication** Not applicable.

**Ethics approval** For human biospecimens, samples were banked during enrollment in clinical trial NCT#04198766 at the Providence Cancer Institute (Portland, Oregon, USA) and signed informed consent before collection under an IRB-approved protocol (#06-108). Participants gave informed consent to participate in the study before taking part.

**Provenance and peer review** Not commissioned; externally peer reviewed.

**Data availability statement** Data are available upon reasonable request. Data are available from the authors upon reasonable request.

**Supplemental material** This content has been supplied by the author(s). It has not been vetted by BMJ Publishing Group Limited (BMJ) and may not have been peer-reviewed. Any opinions or recommendations discussed are solely those of the author(s) and are not endorsed by BMJ. BMJ disclaims all liability and responsibility arising from any reliance placed on the content. Where the content includes any translated material, BMJ does not warrant the accuracy and reliability

of the translations (including but not limited to local regulations, clinical guidelines, terminology, drug names and drug dosages), and is not responsible for any error and/or omissions arising from translation and adaptation or otherwise.

**Open access** This is an open access article distributed in accordance with the Creative Commons Attribution Non Commercial (CC BY-NC 4.0) license, which permits others to distribute, remix, adapt, build upon this work non-commercially, and license their derivative works on different terms, provided the original work is properly cited, appropriate credit is given, any changes made indicated, and the use is non-commercial. See <http://creativecommons.org/licenses/by-nc/4.0/>.

#### ORCID iDs

Nisha Holay <http://orcid.org/0000-0003-4363-3521>

Annah S Rolig <http://orcid.org/0000-0001-7080-4352>

William L Redmond <http://orcid.org/0000-0002-2572-1731>

#### REFERENCES

- Pardoll DM. The blockade of immune checkpoints in cancer immunotherapy. *Nat Rev Cancer* 2012;12:252–64.
- Mayes PA, Hance KW, Hoos A. The promise and challenges of immune agonist antibody development in cancer. *Nat Rev Drug Discov* 2018;17:509–27.
- Walsh RJ, Sundar R, Lim JSJ. Immune checkpoint inhibitor combinations-current and emerging strategies. *Br J Cancer* 2023;128:1415–7.
- Vafaei S, Zekiy AO, Khanamir RA, et al. Combination therapy with immune checkpoint inhibitors (ICIs); a new frontier. *Cancer Cell Int* 2022;22:2.
- Vesely MD, Zhang T, Chen L. Resistance Mechanisms to Anti-PD Cancer Immunotherapy. *Annu Rev Immunol* 2022;40:45–74.
- Ribas A, Wolchok JD. Cancer immunotherapy using checkpoint blockade. *Science* 2018;359:1350–5.
- Croft M. Control of immunity by the TNFR-related molecule OX40 (CD134). *Annu Rev Immunol* 2010;28:57–78.
- Salek-Ardakani S, Croft M. Tumor necrosis factor receptor/tumor necrosis factor family members in antiviral CD8 T-cell immunity. *J Interferon Cytokine Res* 2010;30:205–18.
- Al-Shamkhani A, Birkeland ML, Puklavac M, et al. OX40 is differentially expressed on activated rat and mouse T cells and is the sole receptor for the OX40 ligand. *Eur J Immunol* 1996;26:1695–9.
- Baumann R, Yousefi S, Simon D, et al. Functional expression of CD134 by neutrophils. *Eur J Immunol* 2004;34:2268–75.
- Turaj AH, Cox KL, Penfold CA, et al. Augmentation of CD134 (OX40)-dependent NK anti-tumour activity is dependent on antibody cross-linking. *Sci Rep* 2018;8:2278.
- Weinberg AD, Morris NP, Kovacs-Bankowski M, et al. Science gone translational: the OX40 agonist story. *Immunol Rev* 2011;244:218–31.
- Burocchi A, Pittoni P, Gorzanelli A, et al. Intratumor OX40 stimulation inhibits IRF1 expression and IL-10 production by Treg cells while enhancing CD40L expression by effector memory T cells. *Eur J Immunol* 2011;41:3615–26.
- Gough MJ, Ruby CE, Redmond WL, et al. OX40 agonist therapy enhances CD8 infiltration and decreases immune suppression in the tumor. *Cancer Res* 2008;68:5206–15.
- Pardee AD, McCurry D, Alber S, et al. A therapeutic OX40 agonist dynamically alters dendritic, endothelial, and T cell subsets within the established tumor microenvironment. *Cancer Res* 2010;70:9041–52.
- Valzasina B, Guiducci C, Dislich H, et al. Triggering of OX40 (CD134) on CD4(+)CD25+ T cells blocks their inhibitory activity: a novel regulatory role for OX40 and its comparison with GITR. *Blood* 2005;105:2845–51.
- Vu MD, Xiao X, Gao W, et al. OX40 costimulation turns off Foxp3+ Tregs. *Blood* 2007;110:2501–10.
- Ito T, Wang Y-H, Duramad O, et al. OX40 ligand shuts down IL-10-producing regulatory T cells. *Proc Natl Acad Sci USA* 2006;103:13138–43.
- Ruby CE, Yates MA, Hirschhorn-Cymerman D, et al. Cutting Edge: OX40 agonists can drive regulatory T cell expansion if the cytokine milieu is right. *J Immunol* 2009;183:4853–7.
- Diab A, Hamid O, Thompson JA, et al. A Phase I, Open-Label, Dose-Escalation Study of the OX40 Agonist Ivuxolimab in Patients with Locally Advanced or Metastatic Cancers. *Clin Cancer Res* 2022;28:71–83.
- Kim TW, Burris HA, de Miguel Luken MJ, et al. First-In-Human Phase I Study of the OX40 Agonist MOXR0916 in Patients with Advanced Solid Tumors. *Clin Cancer Res* 2022;28:3452–63.
- El-Khoueiry AB, Spano J-P, Angevin E, et al. Analysis of OX40 agonist antibody (PF-04518600) in patients with hepatocellular carcinoma. *JCO* 2020;38:523.
- Davis EJ, Martin-Liberal J, Kristeleit R, et al. First-in-human phase I/II, open-label study of the anti-OX40 agonist INCAGN01949 in patients with advanced solid tumors. *J Immunother Cancer* 2022;10:e004235.
- Glisson BS, Leidner RS, Ferris RL, et al. Safety and clinical activity of MEDI0562, a humanized OX40 agonist monoclonal antibody, in adult patients with advanced solid tumors. *Clin Cancer Res* 2020;26:5358–67.
- Duhen R, Ballesteros-Merino C, Frye AK, et al. Neoadjuvant anti-OX40 (MEDI6469) therapy in patients with head and neck squamous cell carcinoma activates and expands antigen-specific tumor-infiltrating T cells. *Nat Commun* 2021;12:1047.
- Goldman JW, Piha-Paul SA, Curti B, et al. Safety and tolerability of MEDI0562, an OX40 agonist mAb, in combination with durvalumab or tremelimumab in adult patients with advanced solid tumors. *Clin Cancer Res* 2022;28:3709–19.
- Yadav R, Redmond WL. Current clinical trial landscape of OX40 agonists. *Curr Oncol Rep* 2022;24:951–60.
- Wajant H. Principles of antibody-mediated TNF receptor activation. *Cell Death Differ* 2015;22:1727–41.
- Vanamee ES, Faustman DL. Structural principles of tumor necrosis factor superfamily signaling. *Sci Signal* 2018;11:eaa04910.
- Vanamee ES, Faustman DL. The benefits of clustering in TNF receptor superfamily signaling. *Front Immunol* 2023;14:1225704.
- Glögl M, Krishnakumar A, Ragotte RJ, et al. Target-conditioned diffusion generates potent TNFR superfamily antagonists and agonists. *Science* 2024;386:1154–61.
- Rowell E, Kinkead H, Torretti E, et al. 856 INBRX-106: a novel hexavalent anti-ox40 agonist for the treatment of solid tumors. *J Immunother Cancer* 2021.
- Morris NP, Peters C, Montler R, et al. Development and characterization of recombinant human Fc:OX40L fusion protein linked via a coiled-coil trimerization domain. *Mol Immunol* 2007;44:3112–21.
- Siegemund M, Oak P, Hansbauer E-M, et al. Pharmacokinetic engineering of OX40-blocking anticalin proteins using monomeric plasma half-life extension domains. *Front Pharmacol* 2021;12:759337.
- Koguchi Y, Gonzalez IL, Meeuwse TL, et al. A semi-automated approach to preparing antibody cocktails for immunophenotypic analysis of human peripheral blood. *J Vis Exp* 2016.
- Conrad VK, Dubay CJ, Malek M, et al. Implementation and validation of an automated flow cytometry analysis pipeline for human immune profiling. *Cytometry A* 2019;95:183–91.
- Zhang J, Jiang X, Gao H, et al. Structural basis of a novel agonistic anti-OX40 antibody. *Biomolecules* 2022;12:1209.
- Nguyen TH, Kumar D, Prince C, et al. Frequency of HLA-DR<sup>+</sup>CD38<sup>hi</sup> T cells identifies and quantifies T-cell activation in hemophagocytic lymphohistiocytosis, hyperinflammation, and immune regulatory disorders. *J Allergy Clin Immunol* 2024;153:309–19.
- Saraiva DP, Azeredo-Lopes S, Antunes A, et al. Expression of HLA-DR in Cytotoxic T Lymphocytes: A Validated Predictive Biomarker and a Potential Therapeutic Strategy in Breast Cancer. *Cancers (Basel)* 2021;13:3841.
- Redmond WL, Linch SN, Kasiewicz MJ. Combined targeting of costimulatory (OX40) and coinhibitory (CTLA-4) pathways elicits potent effector T cells capable of driving robust antitumor immunity. *Cancer Immunol Res* 2014;2:142–53.
- Redmond WL, Ruby CE, Weinberg AD. The role of OX40-mediated co-stimulation in T-cell activation and survival. *Crit Rev Immunol* 2009;29:187–201.
- Jensen SM, Maston LD, Gough MJ, et al. Signaling through OX40 enhances antitumor immunity. *Semin Oncol* 2010;37:524–32.
- Linch SN, Redmond WL. Combined OX40 ligation plus CTLA-4 blockade. *Oncoimmunology* 2014;3:e28245.
- Croft M, Salek-Ardakani S, Ware CF. Targeting the TNF and TNFR superfamilies in autoimmune disease and cancer. *Nat Rev Drug Discov* 2024;23:939–61.
- Suntharalingam G, Perry MR, Ward S, et al. Cytokine storm in a phase 1 trial of the anti-CD28 monoclonal antibody TGN1412. *N Engl J Med* 2006;355:1018–28.
- Knorr DA, Dahan R, Ravetch JV. Toxicity of an Fc-engineered anti-CD40 antibody is abrogated by intratumoral injection and results in durable antitumor immunity. *Proc Natl Acad Sci U S A* 2018;115:11048–53.
- Vonderheide RH, Dutcher JP, Anderson JE, et al. Phase I study of recombinant human CD40 ligand in cancer patients. *J Clin Oncol* 2001;19:3280–7.



- 48 Hinterbrandner M, Rubino V, Stoll C, *et al.* Tnfrsf4-expressing regulatory T cells promote immune escape of chronic myeloid leukemia stem cells. *JCI Insight* 2021;6:e151797.
- 49 Linch SN, Kasiewicz MJ, McNamara MJ, *et al.* Combination OX40 agonism/CTLA-4 blockade with HER2 vaccination reverses T-cell anergy and promotes survival in tumor-bearing mice. *Proc Natl Acad Sci U S A* 2016;113:E319–27.
- 50 Emerson DA, Rolig AS, Redmond WL. Enhancing the generation of eomeshi CD8+ T cells augments the efficacy of OX40- and CTLA-4-targeted immunotherapy. *Cancer Immunol Res* 2021;9:430–40.